Conference on Modelling Fluid Flow (CMFF'22)
The 18th International Conference on Fluid Flow Technologies
Budapest, Hungary, August 30 -September 2, 2022

ANALYSIS OF THE REPEAT COLLISION EFFECT IN SIMULATED PARTICLE-LADEN FLOWS WITH AND WITHOUT AGGLOMERATION

David RUPP[1], Lee MORTIMER[2], Michael FAIRWEATHER[3]

[1] Corresponding Author. School of Chemical and Process Engineering, Faculty of Engineering and Physical Sciences, University of Leeds. Leeds LS2 9JT, United Kingdom. E-mail: pmdr@leeds.ac.uk
[2] School of Chemical and Process Engineering, Faculty of Engineering and Physical Sciences, University of Leeds. Leeds LS2 9JT, United Kingdom. E-mail: l.f.mortimer@leeds.ac.uk
[3] School of Chemical and Process Engineering, Faculty of Engineering and Physical Sciences, University of Leeds. Leeds LS2 9JT, United Kingdom. E-mail: m.fairweather@leeds.ac.uk

ABSTRACT

Direct numerical simulation, facilitated by the spectral element method, has been used to study collisions and agglomeration in particle-laden fluid flows through a channel at shear Reynolds number$Re_\tau = 300$. The particulate phase is simulated using Lagrangian particle tracking and a stochastic technique. Curiously, the implementation of agglomeration in the deterministic approach caused a major reduction in the particle collision rate. To determine the cause of this effect, analysis of the collision rate across the channel for different particle properties was performed. For systems without agglomeration, collisions between particles tended to be located on consistent streamlines, occurring between single pairs of particles. A numerical analysis of this effect confirmed the result, where inter-particle collisions across the channel mostly took place between non-unique particle pairs, i.e. particle pairs which collide more than once within a short timeframe. This repeat collision effect was weakest towards the channel walls, and a dependency on the size of the turbulent eddies within the channel was observed. Repeat collisions are shown to be almost eliminated with the addition of the agglomeration mechanism. The impact of this effect on the accuracy of the stochastic technique is discussed, and modifications are suggested to account for the repeat collisions. Even with these the collision rate was exaggerated compared to the deterministic approach.

Keywords: Particle-laden flows, agglomeration, collision, DNS, LPT, stochastic method.

NOMENCLATURE

C_D	[-]	Drag coefficient
C_L	[-]	Lift coefficient
d_p^*	[-]	Particle diameter
e_n^{*2}	[-]	Coefficient of restitution
$\boldsymbol{f}_i$	[-]	Body forces on cell i
$\boldsymbol{f}_{PG}$	[-]	Pressure gradient force
$\boldsymbol{f}_{2W}^{*i}$	[-]	Two-way coupling force
H^*	[-]	Hamaker constant
M_{VM}	[-]	Virtual or added mass term
p^*	[-]	Pressure
P_{coll}	[-]	Collision probability
r_p^*	[-]	Particle radius
Re_B	[-]	Bulk Reynolds number
Re_τ	[-]	Shear Reynolds number
t^*	[-]	Time
u_η	[-]	Kolmogorov velocity scale
$\boldsymbol{u}^*$	[-]	Fluid velocity vector
$\boldsymbol{u}_S^*$	[-]	Slip velocity
$\boldsymbol{u}_F^*$	[-]	Fluid velocity
U_B	[m s^{-1}]	Fluid bulk velocity
V_i^*	[-]	Volume of a computational cell
$\boldsymbol{x}_P^*$	[-]	Particle position
δ	[m]	Channel half-height
δ_0^*	[-]	Minimum contact distance
ε	[m^2 s^{-2}]	Turbulence energy dissipation rate
η	[-]	Kolmogorov length scale
ν	[m^2 s^{-1}]	Kinematic viscosity
ρ_F	[kg m^{-3}]	Fluid phase density
ρ_P	[kg m^{-3}]	Particle phase density
$\boldsymbol{\tau}^*$	[-]	Deviatoric stress tensor
$\boldsymbol{\omega}_F^*$	[-]	Fluid vorticity

Subscripts and Superscripts

DNS	Direct numerical simulation
DSMC	Direct simulation Monte Carlo
LES	Large eddy simulation
LPT	Lagrangian particle tracker
SEM	Spectral element method
x, y, z	Cartesian coordinates
*	Non-dimensional units

1. INTRODUCTION

Accurate simulation of particle-laden flows is of fundamental importance to any area of industry that will at some point be required to transport a fluid-solid multiphase component of its process or waste to a new location. Multiphase flow simulations are frequently performed in industries which refine and transport chemicals, such as agriculture [1], pharmaceuticals [2], and mineral processing [3]. The core electrical energy generation methods, coal, oil and gas, are also obvious examples that handle multiphase flows [4]. Without informed optimisation, industrial processes can be inefficient, unsafe and costly, due to the amount of maintenance required, or the need for part replacement, which can often be hazardous. This is particularly true of the nuclear waste processing industry where exposure to radioactive or otherwise dangerous materials is possible.

The dynamic properties and complex mechanisms of turbulent wall-bounded flows demand high levels of mathematical accuracy for the purpose of making predictions of chaotic behaviour. A minute change in initial conditions will inextricably lead to differing results. In the case of experimental studies, this sensitivity to initial conditions can lead to unreliable reproducibility, for said conditions are tremendously difficult to isolate, more so as the Reynolds number increases. For a more accurate representation of the flow, methods such as large eddy simulation (LES) and direct numerical simulation (DNS) are available. Both of these methods involve constructing a mesh for resolving small scale effects with high accuracy, and then solving the Navier-Stokes equations at all the relevant scales.

Traditionally, the Lagrangian particle tracking method has been used to simulate the movement of particles and the collisions thereof. In this case, particles are modelled as computational spheres and a suitably integrated force-balance equation of motion is used to advect them. This method, whilst accurate, suffers from similar computational constraints to DNS, where collision calculations become unfeasible for large particle numbers, often required for the representation of industrial flows.

One alternative to the Lagrangian method of colliding particles is the stochastic method [5], for which complexity scales with the number of particles, rather than the number squared. The method calculates the likelihood of a particular particle colliding through the generation of a fictitious collision partner, which is representative of the local particle phase properties, so that no information is required on the actual position and direction of motion of the surrounding real particles [5]. This then resolves the correct number of collisions for the flow based on the collision probability and the averaged statistics of the particles in the same region.

This study investigates this methodology in conjunction with a channel flow geometry where both inter-particle collisions and agglomeration are considered. It assesses an unexpected condition that the implementation of agglomeration causes, with the stochastic method, an excessively high collision rate, and determines a cause and potential solution.

2. METHODOLOGY

To simulate the continuous phase, a spectral element method (SEM) is used to determine the action of the fluid. The SEM is a hybrid of the finite element method and the spectral method. Combining the accuracy of the spectral method with the generality of the finite element method leads to a much more flexible technique for solving the incompressible Navier-Stokes equations. The code employed, Nek5000 [6], has been extensively tested and validated, and contains efficient parallelisation capabilities as well as the flexibility to include an effective particle phase model. The SEM is implemented by dividing the fluid domain into smaller elements, the number and shape of which are determined by the geometry of the domain and by the intended resolution of the program, with enough flexibility to accommodate common and indeed uncommon fluid domains. This work used DNS, so the elements used have an upper bound for size, which is ideally no greater than 15 times the Kolmogorov length scale [7]. The non-dimensionalised Navier-Stokes equations can be stated as:

$$\frac{d\boldsymbol{u}^*}{dt^*} + (\boldsymbol{u}^* \cdot \nabla)\boldsymbol{u}^* = -\nabla p^* + \frac{1}{Re_B}\nabla \cdot \boldsymbol{\tau}^* + f_i \qquad (1)$$

$$\nabla \cdot \boldsymbol{u}^* = 0 \qquad (2)$$

Here, $\boldsymbol{u}^*$ is the fluid velocity vector, which has been non-dimensionalised in terms of the bulk velocity U_B, and t^* is an expression of non-dimensionalised time, $t^* = tU_B/\delta$, where δ is half the height of the channel. p^* is a non-dimensionalised pressure term, $p^* = p/\rho_F {U_B}^2$, where ρ_F is the density of the continuous phase. Re_B is the bulk Reynolds number given by $\delta U_B/v$, and $\boldsymbol{\tau}^*$ is the non-dimensionalised deviatoric stress tensor, $\boldsymbol{\tau}^* = (\nabla \boldsymbol{u}^* + \nabla \boldsymbol{u}^{*T})$. The final term, f_i, represents body forces on cell i, given by $\boldsymbol{f}_i = \boldsymbol{f}_{PG} + \boldsymbol{f}_{2W}^{*i}$. The flow is driven by a constant pressure gradient term $\boldsymbol{f}_{PG} = (Re_\tau/Re_B)^2\hat{\boldsymbol{x}}$, with $\hat{\boldsymbol{x}}$ a unit vector in the streamwise direction. The term $\boldsymbol{f}_{2W}^{*i}$ represents two-way momentum exchange between the fluid and particulate phases.

These equations were solved by Nek5000 for an initially turbulent fluid flow in a channel geometry of $12 \times 2 \times 6$ non-dimensional distance units where the 12 (x^*) and 6 (z^*) dimensions had continuous, periodic boundaries, and the 2 (y^*) dimension was

wall-bounded with a no-slip condition. At $Re_\tau = 300$ this was simulated using a $32 \times 32 \times 32$ element mesh with spectral discretization order $N = 7$, i.e. a total of 11.2M elements.

In order to model the dispersed particle phase of a multiphase flow, a Lagrangian particle tracker (LPT) was first employed which was developed in conjunction with the Nek5000 code used in this study. The Lagrangian particle tracking routine tracks individual particles as computational spheres, and time-evolves their velocity and position synchronously with the Eulerian fluid flow model, operating over the same timesteps and representing the fluid-particle interactions by solving the non-dimensional equations of motion described below:

$$\frac{\partial \boldsymbol{x}_P^*}{\partial t^*} = \boldsymbol{u}_P^* \tag{3}$$

$$\frac{\partial \boldsymbol{u}_P^*}{\partial t^*} = \frac{1}{M_{VM}} \left[\underbrace{\frac{3 C_D |\boldsymbol{u}_s^*|}{4 d_p^* \rho_P^*} \boldsymbol{u}_s^*}_{Drag} + \underbrace{\frac{3}{4} \frac{C_L}{\rho_P^*} (\boldsymbol{u}_s^* \times \boldsymbol{\omega}_F^*)}_{Lift} + \underbrace{\frac{1}{2 \rho_P^*} \frac{D \boldsymbol{u}_F^*}{D t^*}}_{Virtual\ Mass} + \underbrace{\frac{1}{\rho_P^*} \frac{D \boldsymbol{u}_F^*}{D t^*}}_{Pressure\ Gradient} \right] \tag{4}$$

The fourth order Runge-Kutta method, also known as RK4 [8], was used to solve these equations for each particle within every time-step in the Lagrangian particle tracker. Here, d_p^* and ρ_P^* are respectively the diameter and density of the particle, and, after being non-dimensionalised, $\boldsymbol{u}_s^*$, $\boldsymbol{u}_F^*$ and $\boldsymbol{\omega}_F^*$ are the slip velocity, fluid velocity and vorticity, with C_D and C_L being the coefficients of drag and lift.

For increased volume fraction flows where collision effects are dominant, the effect of the particles on the fluid must be considered. The two-way coupling momentum exchange term is included in the final term of Eq. (1) to account for this:

$$\boldsymbol{f}_{2W}^{*i} = \frac{1}{V_i^*} \sum_j \frac{\partial \boldsymbol{u}_{P\,j}^*}{\partial t^*} \tag{5}$$

where V_i^* is the volume of a computational cell, and j is a function applied to each particle in that cell.

The deterministic particle interactions were treated as hard sphere collisions, with collision times smaller than the LPT timestep, and additional interparticle forces were either ignored as negligible, or partially implemented as part of the agglomeration mechanism. To reduce computational demand, the domain was reduced into smaller cells, with only particles in the same cell considered as potential collision partners. The non-dimensional radii of the particles considered in this study were $r_p^* = 0.005$ and 0.01 (equivalent to 100 μm and 200 μm particles, with Stokes numbers, in water, of 0.31 and 1.25, respectively) .

A deterministic energy-balance method was used to calculate the energetic collision conditions under which an agglomerate forms, as used by Njobuenwu and Fairweather [9]. This is given as:

$$\boldsymbol{u}_{P,rel}^{*2} - \frac{(1 - e_n^{*2}) \left(\boldsymbol{u}_{P,rel}^* . \hat{\boldsymbol{n}} \right)^2}{\left| \left(\boldsymbol{u}_{P,rel}^* . \hat{\boldsymbol{n}} \right) \right|} \leq \frac{H^*}{6 \delta_0^{*2}} \left[\frac{6(1 - e_n^{*2})}{\pi^2 \rho_P^* \sigma^*} \left(\frac{d_{P,i}^{*3} + d_{P,j}^{*3}}{d_{P,i}^{*2} d_{P,j}^{*2} \left(d_{P,i}^* + d_{P,j}^* \right)} \right) \right} \tag{6}$$

where H^* is the non-dimensional Hamaker constant, given by $H^* = H / \rho_F U_B^2 \delta^3$, $\delta_0^* = \delta_0 / \delta$ is the minimum contact distance, also non-dimensionalised, and e_n^{*2} is the normal coefficient of restitution. $\hat{\boldsymbol{n}}$ is a unit vector pointing between the colliding particle pair and $\boldsymbol{u}_{P,rel}^{*2}$ is the relative velocity between the colliding particles. Upon collision, if the condition stated in the equation is satisfied, the particles are considered to combine into a spherical agglomerate with radius calculated such that the new volume is equivalent to the summed volume of its constituents.

Rupp et al. [10] introduced a modified stochastic technique for use in channel flows, which employs advective theory as derived by Saffman and Turner [11]. This calculates the particle collision rate within a given strata of a flow, a cell encompassing the entirety of the channel in the streamwise and spanwise dimensions, and a small section in the wall-normal dimension, matching the fluid elements used. The probability of collision for a particle is given as:

$$P_{coll} = \left(\frac{8\pi}{15} \right)^{1/2} n_p (d_p)^3 \left(\frac{\varepsilon}{\nu} \right)^{1/2} \Delta t \tag{7}$$

where ε is the turbulence kinetic energy dissipation rate, ν is the kinematic viscosity, and n_p and d_p are the particle number density and the diameter. Two classes of particle were simulated using both the deterministic and stochastic techniques. Further simulations were perfomed for both cases with the agglomeration mechanism active. As will be made apparent in the discussion section, modifications were required to be made to the code where the stochastic technique was employed in a model with agglomeration. These modifications were based on observations made by Wang et al. [12], where the below equation relates to the change in the collision rate due to certain interparticle effects such as the accumulation effect:

$$\frac{\Gamma}{\Gamma_0} = 4.85 \frac{\eta}{r} g(r) \frac{\langle |w_r| \rangle}{u_\eta} \tag{8}$$

Here, η and u_η represent, respectively, the Kolmogorov length and velocity scales, r is the radius, and $g(r)$ is a statistical function of the radius known as the radial distribution at contact which directly measures the accumulation effect. $\langle|w_r|\rangle$ represents the Lagrangian pair relative velocity statistics of particles and is a measure of the turbulent transport effect.

3. RESULTS AND DISCUSSION

The baseline case for this study was a four-way coupled deterministic simulation of a turbulent channel flow without agglomeration. This was performed for particles of radii $r_p^* = 0.005$ and 0.01 at quantities of 300k and 2.2M. The results of these simulations were previously compared with the outcomes using the direct simulation Monte Carlo (DSMC) stochastic technique, showing good agreement [10]. Simulations using the agglomeration mechanism generated useful results surrounding both the impact of particles on the fluid as well as the rate of particulate aggregation in simple wall-bounded flows. In general, the effect of agglomeration on the mean fluid streamwise velocities and the normal and shear stresses was small over the simulation time considered. Of the cases considered, the system with the most significant change was the channel populated with the higher radius $r_p^* = 0.01$ particles, with results shown in Figs. 1 and 2.

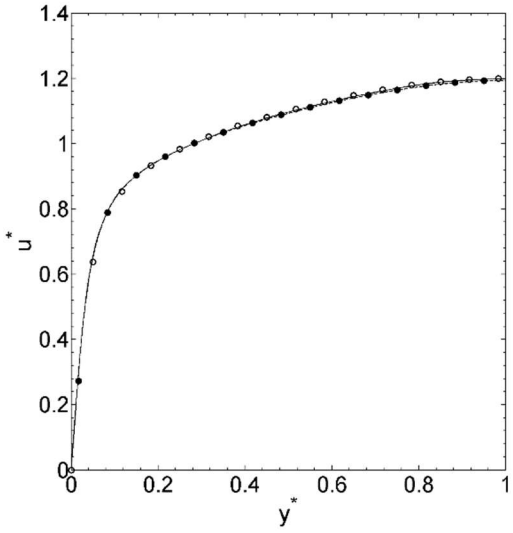

Figure 1. Mean streamwise velocities, u^*, for fluid flows with 300k, 200µm particles. Fluid values from the simulation — with and - - - without agglomeration, and particle values ● with and ○ without agglomeration.

The inclusion of high Stokes number particles can be seen to have affected the overall particle statistics slightly, and the fluid statistics less so (with little difference visible between the lines with and without agglomeration). Previous studies by the authors in this geometry and Reynolds number have shown the mean streamwise velocity to be resistant to change, and likewise here the streamwise particle velocity shown in Fig. 1 is seen to be minimally impeded towards the centre of the channel.

The normal and shear stresses, displayed in Fig. 2, are likewise minimally affected. A notable change is in the spanwise fluid velocity at $0.3 < y^* < 0.7$, a region shown in previous studies to be particularly affected by changes in the particle Stokes number [13].

Figure 3 is a plot of the evolution of agglomerates over time for the high concentration case (where aggregation is most significant), and demonstrates the formation of agglomerates containing as many as 40 single particles by $t^* = 150$. Thus, the lines, ranging from top to bottom in the plot, are for single particles, and then for agglomerates with 2, 3, 4 ... 10 particles, followed by particles with 15, 20 ... 40 particles.

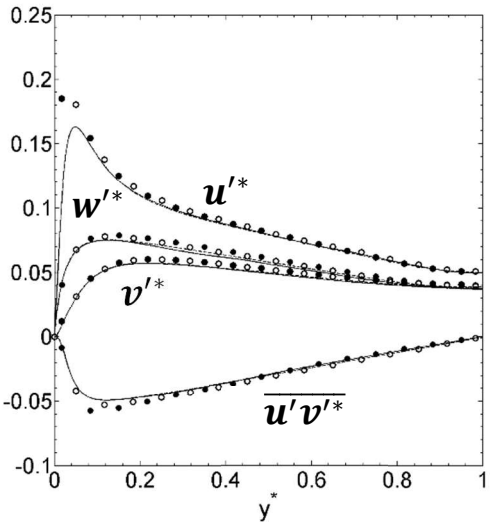

Figure 2. Normal and shear stresses, $u'^*, v'^*, w'^*, \overline{u'v'^*}$, for fluid flows with 300k, 200µm particles. Fluid values from the simulation — with and - - - without agglomeration, and particle values ● with and ○ without agglomeration.

Having demonstrated the DSMC stochastic technique for the prediction of collisions in previous work, the model was now incorporated into the overall model which employed the additional post-collision agglomeration mechanism. However, this resulted in an immediate upturn in agglomeration when compared to the deterministic interaction flow, to the point where the simulation could not handle the effects on the fluid flow from the sudden appearance of many high Stokes number particles created by agglomeration.

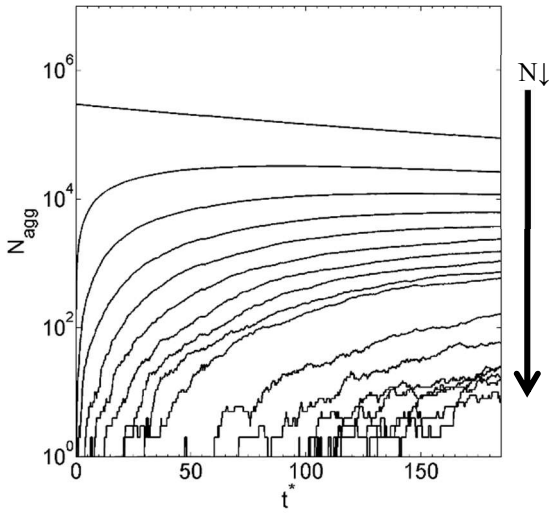

Figure 3. Number, N_{agg}, of differently sized agglomerates for 2.2M, 100µm deterministic particles with sizes N = 1, 2, 3 … 9 and 10, 15, … 50 (top to bottom).

Since the stochastic technique had up to this point been consistent with the deterministic as far as the collision rate was concerned, this effect was of interest. It was initially theorised to be because of an underestimation in the collision energy, or some other peculiarity of the stochastic technique. Even a small change in collision rate would quickly accumulate to a large change in the effects of agglomeration, and the stochastic technique did exhibit an increased collision rate compared to the deterministic approach. This increase was further determined to be a small part of the effect. What was quickly ascertained was that the collision rate dropped substantially when agglomeration was implemented for the deterministic simulation of particles, with Table 1 showing the scale of this decrease to be of at least an order of magnitude.

Investigating the cause of the change in collision rate was carried out through analysis of the collision location within the channel. The locations of collisions taking place over the course of 100 simulation timesteps were recorded and are illustrated in Fig. 4. For the purpose of easier visualisation, a sector of the channel was chosen that was one half of the total length, width and breadth of the entire geometry.

Each individual point in the figure represents the location of a collision between two particles. These positions tend to form dotted lines, particularly towards the centreline of the channel. These would appear to indicate multiple collisions occurring in the same relative places over the course of the simulation. The fact that these lines follow fluid streamlines is indicative of this, and indeed what is being observed here is particles that are confined to the same fluid eddies colliding with each other repeatedly.

Table 1. Comparisons of deterministic collision rates per bulk time unit for cases with and without agglomeration.

Case	$300k, r_p^* = 0.005$	$2.2M, r_p^* = 0.005$	$300k, r_p^* = 0.01$
Collisions without agglomeration	2,218	160,847	10,447
Collisions with agglomeration	214	10,299	1,707

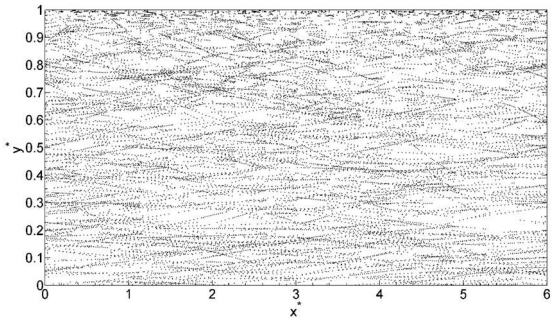

Figure 4. Visualisation of the location (plotted as dots) of deterministic collisions in the $x^* - y^*$ plane for a section of a channel flow in which the 300k, 100µm particle case is being simulated with four-way coupling.

A numerical analysis of this effect was performed, shown in Fig. 5. The identities of the two particles colliding were recorded for a selection of collisions from the deterministic simulation without agglomeration, for the three different cases considered over a hundred timesteps. A unique collision here is defined from these identities, counted as the first time a particular pair of particles had collided during those timesteps.

Comparing the numbers of unique collisions across the channel to the total number within that section showed that the majority of non-unique collisions (shown in Fig. 5) take place at the centre of the channel, where the turbulent eddies are most stable. The simulation with the lowest radius and particle number had the lowest collision rate overall, and this makes it something of an outlier, with non-unique collisions being far more likely to occur than for any two given particles to encounter each other for the first time.

The $r_p^* = 0.01$ case also has some unique properties, with an increase in non-unique collisions in the wall regions. This is caused by turbophoresis moving high speed particles to those regions. Overall, a higher collision rate caused by either particle size or number increasing has the effect of

increasing the rate of unique collisions, though the collision rate is still dominated by particles that are kept in close proximity by localised fluid effects.

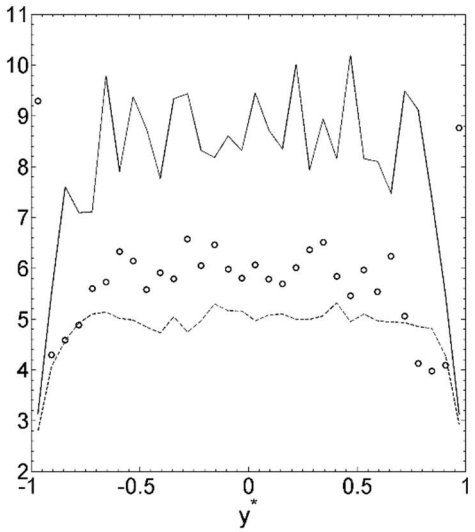

Figure 5. Proportion of deterministic collisions taking place across the channel which are not unique for three particle cases simulated in this study. — $N_p = 300k, r_p^* = 0.005$; - - - $N_p = 2.2M, r_p^* = 0.005$; ○ $N_p = 300k, r_p^* = 0.01$.

Particles under these conditions, due to continuous proximity and repeated chances for collision, would agglomerate with greater frequency when this is considered as a factor in the simulation. With the existence of particles in similar local fluid regions becoming a non-factor, the collision rate drops quickly and stabilises at a much lower value than predicted by the four-way coupled simulation without agglomeration. This can be seen in Fig. 6, which shows the collision rate over time.

Here, each case displays an initial spike of collisions. This is an artifact of the initial conditions, which took particle statistics from an already settled flow without agglomeration, but illustrates an effect larger than the reduction in collision rate over time as more and more particles agglomerate. The case with the large radius particles is the only one where the collision rate changes comparably.

The stochastic simulation of the four-way coupled system, however, considers only the advective forces on the particles, and their sizes in the calculation of collision rate. This does not quickly change with the implementation of agglomeration, and as a result the collision rate remains a close match to the first set of values in Table 1, rather than the correct second set. This in turn results in a high agglomeration rate that swiftly results in absurdly large particles and makes the simulation of limited value.

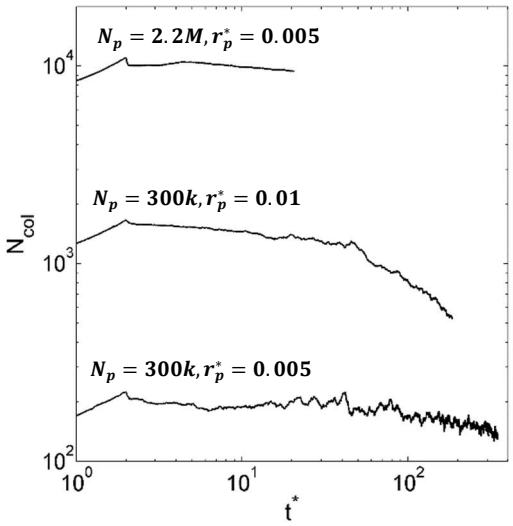

Figure 6. Temporal evolution of number of collisions per timestep for the three deterministic cases colliding with agglomeration.

Wang et al. [12] described the effects known as the accumulation effect and the turbulent transport effect. These were potential candidates for the cause of the repeat collision effect that has been observed in this study, so calculations for the magnitude of these effects were implemented into the formulas the stochastic technique uses for the collision rate. This had the desired effect of reducing the rate of collision, and therefore agglomeration, but as Figs. 7 and 8 show, this reduction was not equal to the size of the effect.

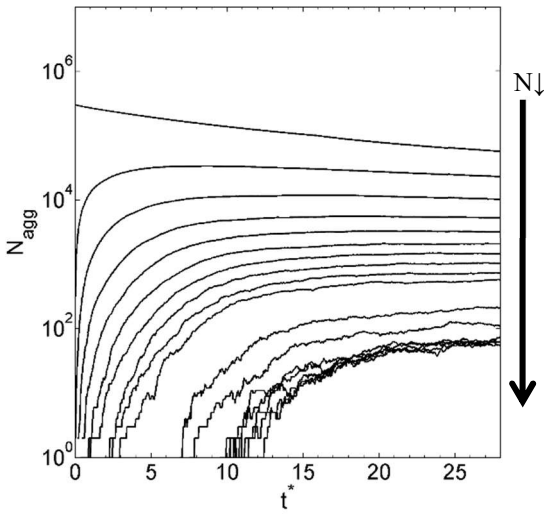

Figure 7. Number, N_{agg}, of differently sized agglomerates for 2.2M, 100μm stochastic particles with sizes N = 1, 2, 3 … 9 and 10, 15, … 50 (top to bottom).

Here it can be seen that even the "improved" stochastic technique is still overpredicting the

collision rate, with the size 40 agglomerates occurring at around $t^* = 10$, rather than $t^* = 150$ as occurred for the corresponding deterministic case in Fig. 3.

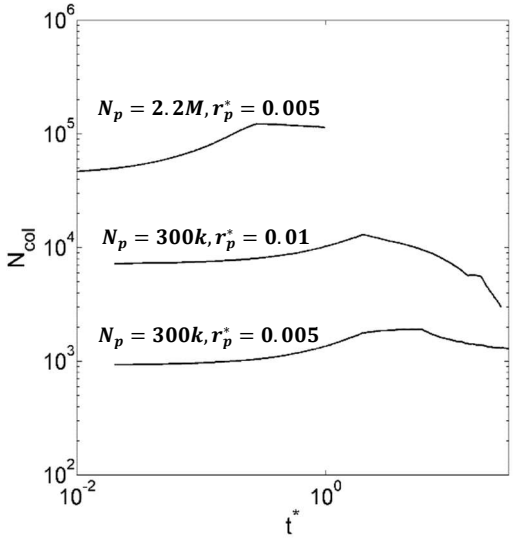

Figure 8. Temporal evolution of number of collisions per timestep for the three stochastic cases colliding with agglomeration.

For the higher concentration case the agglomeration rate was significant enough that the timestep had to be reduced substantially for the simulation to not diverge due to high-Stokes number particle interaction with the fluid. This is why the logarithmic time axis starts earlier for the high concentration case in Fig. 8.

Table 2. Comparisons of deterministic and stochastic runtimes and collision rates for cases with and without agglomeration.

Case	$300k, r_p^* = 0.005$	$2.2M, r_p^* = 0.005$	$300k, r_p^* = 0.01$
Deterministic runtime	2.43	17.75	3.09
Deterministic collisions/t*	214	10,299	1,707
Stochastic runtime	2.19	13.41	2.53
Stochastic collisions/t*	1,895	72,862	15,291

Table 2 shows the collision rates for the modified stochastic technique to be less than an order of magnitude greater, which is an improvement over the unmodified technique, however there is still a clear need for improvement.

The stochastic technique does however reduce the computational demand as claimed, shown in the same table, where the compute time/timestep is normalised by a one-way coupled simulation of the $300k, r_p^* = 0.005$ case. Each case studied was faster where the stochastic technique was used, meaning that further improvements to the technique can be expected to pay dividends in simulation time.

4. CONCLUSIONS

This study investigated the impact of stochastic particle agglomeration on previously studied four-way coupled particle-laden channel flows, with a focus on a repeated collision effect which cause inaccuracies in the agglomeration rate. With agglomeration implemented, the simulation of particle-laden channel flows gains versatility, in that aggregation can be captured. For this particular geometry and the particles Stokes numbers considered, the effect of the particles on the fluid was small, with the most significant results, from the higher Stokes number case, shown here.

While applying the agglomeration mechanism to a previously successful stochastic DSMC technique, an inconsistency emerged which led to an investigation into what is termed the repeat collision effect. This effect turned out to be a direct result of fluid streamlines in the bulk flow confining low Stokes number particles to close proximity, which would then collide repeatedly, skewing the number of reported collisions.

The stochastic technique, previously observed to match this reported number of collisions, did not account for the agglomeration of the confined particles, leaving isolated agglomerates with a magnitude lower collision rate. It therefore agglomerated particles at an inordinate rate with a devastating effect on the accuracy of the simulation.

An attempt was made to rectify this through modifications based on a study of the accumulation and turbulent transport effects, and this had some success, reducing the collision and agglomeration rates, though not enough to make the simulation accurate.

As improvements to the stochastic technique for handling inter-particle collisions are ongoing, it is expected that further work on this technique will lead to a more effective solution to the repeat collision effect. In the meantime, the stochastic technique has proven an effective way to reduce computational cost in cases where its inconsistencies can be resolved.

Further work also needs to consider the relationship between the coefficient of restitution and the repeat collision effect, as the agglomeration chance per collision was near to unity for this study, and this is what drove the deviations between collision rates with and without agglomeration.

ACKNOWLEDGEMENTS

D.R. would like to thank the Engineering and Physical Sciences Research Council in the UK, and the National Nuclear Laboratory, who funded the work described as part of the EPSRC Centre for Doctoral Training in Nuclear Fission – Next Generation Nuclear.

REFERENCES

[1] Lee, I. B., Bitog, J. P. P., Hong, S.W., Seo, I. H., Kwon, K. S., Bartzanas, T., Kacira, M., 2013, "The past, present and future of CFD for agro-environmental applications." *Computers and Electronics in Agriculture*, Vol. 93, pp. 168-183.

[2] Chakravarti, A., Patankar, N. A., Panchagnula, M. V., 2019, "Aerosol transport in a breathing alveolus." *Physics of Fluids*, Vol. 31, 121901.

[3] Guha, D., Ramachandran, P.A., Dudukovic, M. P., 2007, "Flow field of suspended solids in a stirred tank reactor by Lagrangian tracking." *Chemical Engineering Science*, Vol. 62, pp. 6143-6154.

[4] Raynal, L., Augier, F., Bazer-Bachi, F., Haroun, Y., Pereira da Fonte, C., 2016 "CFD applied to process development in the oil and gas industry – A review." *Oil & Gas Science and Technology*, Vol. 71, 42.

[5] Sommerfeld, M., 2001, "Validation of a stochastic Lagrangian modelling approach for col nter-particle collisions in homogeneous isotropic turbulence", *International Journal of Multiphase Flow*, Vol. 27, pp. 1829-1858.

[6] Fischer, P. F., Lottes, J. W., Kerkemeier, S. G., 2008, Nek5000. http://nek5000.mcs.anl.gov.

[7] Moser, R. D., Moin, P., 1984, "Direct numerical simulation of curved turbulent channel flow." *NASA Technical Memorandum* 85974

[8] Süli, E., Mayers, D., 2003, *An Introduction to Numerical Analysis*, Cambridge University Press.

[9] Njobuenwu, D.O., Fairweather, M., 2017, "Simulation of deterministic energy-balance particle agglomeration in turbulent liquid-solid flows." *Physics of Fluids*, Vol. 29, 083301.

[10] Rupp, D. A., Mortimer, L. F., Fairweather, M., 2021, "Development of an effective stochastic collision method for use in four-way coupled turbulent flows." Proc. *13th International ERCOFTAC Symposium on Engineering Turbulence Modelling and Measurements*, Rhodes, Greece, Paper 13.

[11] Saffman, P. G., Turner, S. J., 1956, "On the collision of drops in turbulent clouds." *Journal of Fluid Mechanics*, Vol. 1, pp. 16-30.

[12] Wang, L. P., Wexler, A. S, Zhou, Y., 2000, "Statistical mechanical description and modelling of turbulent collision of inertial particles." *Journal of Fluid Mechanics*, Vol. 415, pp.117-153.

[13] Rupp, D. A., Njobuenwu, D. O., Fairweather, M., 2018, "Particle volume fraction effects in simulations of turbulent channel flows." In: Proc. *12th International ERCOFTAC Symposium on Engineering Turbulence Modelling and Measurements*, Montpellier, France.